

Brownian thermal birefringent noise due to non-diagonal anisotropic photoelastic effect in multilayer coated mirrors

Yu-Pei Zhang,¹ Shi-Xiang Yang,¹ Wen-Hai Tan,^{2,*} Cheng-Gang Shao,¹ Yiqiu Ma,^{1,†} and Shan-Qing Yang²

¹MOE Key Laboratory of Fundamental Physical Quantities Measurement, School of Physics, Huazhong University of Science and Technology, Wuhan 430074, People's Republic of China

²MOE Key Laboratory of TianQin Mission, TianQin Research

Center for Gravitational Physics & School of Physics and Astronomy,

Frontiers Science Center for TianQin, Gravitational Wave Research Center of CNSA,

Sun Yat-sen University (Zhuhai Campus), Zhuhai 519082, People's Republic of China

Thermal noise in the mirror coatings limits the accuracy of today's most optical precision measurement experiments. Unlike the more commonly discussed thermal phase noise, the crystalline coating can generate thermal birefringent noise due to its anisotropic nature. In this study, we propose that the non-diagonal anisotropic photoelastic effect induced by the Brownian motion of mirror coating layers may contribute to this noise. Employing a standard model for the coating surface, we calculate the spectrum of the non-diagonal anisotropic Brownian photoelastic (NABP) noise to be $1.2 \times 10^{-11} p_{63} f^{-1/2} / \text{Hz}^{1/2}$. Further experiments are warranted to validate the influence of this effect and reduce its uncertainty. Our findings highlight that for high-precision experiments involving optical resonant cavities targeting signals imprinted in optical polarizations, this noise could emerge as a limiting factor for experimental sensitivity.

I. INTRODUCTION

The investigation of thermal noise in multilayer-coated mirrors is crucial for understanding its impact on the sensitivity of high-precision measurement experiments conducted within optical resonant cavities. Prominent examples include laser interferometer gravitational-wave detectors [1–5] and optical clocks [6–11]. While the thermal noises in these experiments have traditionally centered on the optical phase effect, extensively explored in prior studies [7, 12–14], we direct attention to experiments involving signals imprinted on the polarization of light, such as the measurement of vacuum magnetic birefringence (VMB) [15–19], or the search for axion-like particles [20–22], where thermal birefringent noise emerges as a key factor.

Low-loss mirrors are constructed by sequentially depositing two different materials onto the substrate, resulting in thermal noise contributed by the coating, the substrate, and by their interface. Here the coating is the main contributor because that optical field is circulated within the cavity by reflecting from the coating layers. Coating thermal noise has two potential sources: (1) temperature variations due to thermal dissipation and (2) Brownian motion due to mechanical dissipation. Due to their low mechanical losses, crystalline coatings have lower Brownian noise than amorphous coatings [23, 24]. However, due to the anisotropic nature of the crystalline coating, its optical properties may exhibit an *anisotropy* which is different from that of the amorphous coatings.

Recent investigations into polarization fluctuations resulting from temperature fluctuations and the *anisotropic*

thermal properties of crystalline coating materials, so called thermorefringent noise, have been reported [25]. Previous studies [26, 27] have considered the photoelastic effect due to Brownian motion in the coating layers, but included only the *isotropic* part which is the diagonal terms in the photoelastic coefficients matrix (i.e., $p_{ij} = p\delta_{ij}$). The optical *anisotropy* produced by the photoelastic effect can be divided into two types. The first one is due to the the unequal diagonal elements which produces the birefringence, and this effect has been studied [16] previously. The other one is due to the the non-diagonal elements, which leads to the variation in the angle of birefringence (see Section II A), which remains unexplored. In this work, we will explore the possible Brownian noise contributed by the non-zero off-diagonal photoelastic coefficients, which could result from the strains induced during the manufacturing process.

Brownian motion of the coating layer, through the non-diagonal anisotropic photoelastic effect, can lead to fluctuations in the polarization state. This noise will appear in the polarization mode that is perpendicular to the incident polarization, termed in this paper as non-diagonal anisotropic Brownian photoelastic (NABP) noise. This noise has the potential to limit the performance of VMB experiments and other precision optical polarization measurement experiments. Therefore, experimental characterisation of the off-diagonal photoelastic coefficient of the coating materials is necessary for an accurate assessment of the NABP noise.

This paper is structured as follows: In Section II, we begin by introducing the theoretical model of the photoelastic effect and its impact when light traverses an anisotropic photoelastic medium. Subsequently, we give the expression for the polarization fluctuations of the reflected light employing the standard structure of mirror coating. In Section III, the noise level of the thermal birefringent noise contributed by the non-diagonal

* tanwh7@mail.sysu.edu.cn

† myqphy@hust.edu.cn

anisotropic photoelastic effect is calculated and compared with other noise. Finally, Section IV summarizes our principal findings and engages in a about future avenues of research.

II. THEORETICAL MODEL

A. Photoelastic effect

The photoelastic effect, denoting the change in refractive index induced by mechanical strain, is characterized by symmetric tensors representing the strain (u_{ij}) and the change in the optical indicatrix (ΔB_{ij}). Utilizing contracted indices ($i, j \in xx, yy, zz, yz, zx, xy$ rather than x, y, z) for these tensors, the photoelastic effect can be expressed in a vectorial form:

$$\Delta B_i = p_{ij}u_j, \quad (1)$$

where ΔB_i is the change of the optical indicatrix, p_{ij} is photoelastic tensor, u_j is strain components (we follow the conventions used in [28] where the six independent matrix elements of u_{ij} is summarized as one vector u_j , the same for the relationship between the ΔB_{ij} and the ΔB_i). Since fluctuations caused by photoelastic effect in the transverse direction are much smaller than in the longitudinal direction [14], we only consider the variation of the refractive index caused by the change of coating thickness

$$\Delta B_i = p_{i3}\delta d/d, \quad (2)$$

where $\delta d/d$ denotes the change in coating thickness. Since light propagates along the z -axis (see Fig.1), and the optical field is confined to the x - y plane, the optical indicatrix \mathbf{B} is given by:

$$\mathbf{B} = \begin{bmatrix} B_{xx} & 0 \\ 0 & B_{yy} \end{bmatrix} + \begin{bmatrix} p_{13} & p_{63} \\ p_{63} & p_{23} \end{bmatrix} \frac{\delta d}{d}, \quad (3)$$

while the dielectric tensor $\boldsymbol{\varepsilon}$ is inverse of \mathbf{B} . To the first order of $\delta d/d$, the dielectric tensor reads:

$$\boldsymbol{\varepsilon} = \mathbf{B}^{-1} \quad (4)$$

$$= \begin{bmatrix} \langle n_x^2 \rangle & 0 \\ 0 & \langle n_y^2 \rangle \end{bmatrix} - \begin{bmatrix} p_{13} \langle n_x^4 \rangle & p_{63} \langle n_x^2 \rangle \langle n_y^2 \rangle \\ p_{63} \langle n_x^2 \rangle \langle n_y^2 \rangle & p_{23} \langle n_y^4 \rangle \end{bmatrix} \frac{\delta d}{d},$$

where $\langle n_x \rangle, \langle n_y \rangle$ is refractive index in x, y direction, $\langle n_x \rangle = B_{xx}^{-1/2}$, $\langle n_y \rangle = B_{yy}^{-1/2}$. The strain variation $\delta d/d$ changes the principle directions of the dielectric tensor, where the refractive index and the new principle directions are given by the diagonalisation of $\boldsymbol{\varepsilon}$:

$$n_x \approx \langle n_x \rangle - \frac{p_{13} \langle n_x^3 \rangle \delta d}{2d}, \quad (5)$$

$$n_y \approx \langle n_y \rangle - \frac{p_{23} \langle n_y^3 \rangle \delta d}{2d}, \quad (6)$$

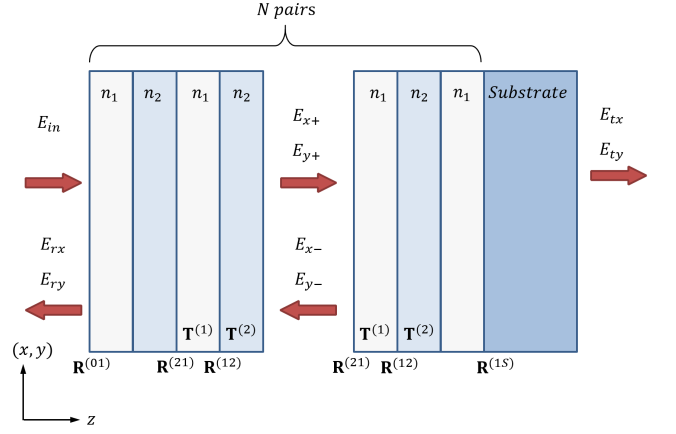


FIG. 1: Structure of multilayer coated mirror. Light colored part represents coating layer, dark colored part represents substrate. The subscript 1 represents GaAs layers and 2 represents AlGaAs layers in our experiments. The thickness of all coating layer is $\lambda/4$ except the first one, which is $\lambda/2$.

with corresponding eigenvectors

$$\mathbf{v}_1 \approx \begin{bmatrix} 1 \\ 0 \end{bmatrix} - \frac{p_{63} \langle n_x^2 \rangle \langle n_y^2 \rangle \delta d}{\langle n_x^2 \rangle - \langle n_y^2 \rangle d} \begin{bmatrix} 0 \\ 1 \end{bmatrix}, \quad (7)$$

$$\mathbf{v}_2 \approx \begin{bmatrix} 0 \\ 1 \end{bmatrix} + \frac{p_{63} \langle n_x^2 \rangle \langle n_y^2 \rangle \delta d}{\langle n_x^2 \rangle - \langle n_y^2 \rangle d} \begin{bmatrix} 1 \\ 0 \end{bmatrix}. \quad (8)$$

This fluctuations in eigenvectors is equivalent to intrinsic birefringence of coating rotated by a small angle

$$\delta\theta \approx -\frac{p_{63} \langle n_x^2 \rangle \langle n_y^2 \rangle \delta d}{\langle n_x^2 \rangle - \langle n_y^2 \rangle d}. \quad (9)$$

Notably, while the influence of p_{13} and p_{23} on fluctuations in n_x and n_y has been previously studied [26], the impact of the p_{63} term, leading to fluctuations in the angle of intrinsic birefringence, remains unexplored.

Typical optical materials used in the crystalline coating are GaAs/AlGaAs. Theoretically both materials are isotropic and therefore do not have non-diagonal photoelastic coefficients p_{63} . Here we propose two possible physical scenarios for producing a non-zero p_{63} . Since the thermal expansion coefficients of the coating α_C and the substrate α_S are different, the thermal elasticity will induce a strain in the coating layers when the temperature drops from the manufacturing temperature to the room temperature [29]:

$$\frac{\delta l}{l} = (\alpha_C - \alpha_S)\Delta T = 2 \times 10^{-3} \quad (10)$$

Theoretically, the coating film is stressed uniformly, which means that the lattices on the coating surface are all exposed to the same stresses, and the direction of the stress is along their location to the centre of the mirror. For most of the lattices on the coating surface, the direction of the crystal axis and the stress are different. This

lowers the symmetry of the crystal system from cubic to monoclinic or triclinic [30], thus producing a non-zero p_{63} .

Another possible mechanism is that the deformation of the top layer is less than that of the layer closest to the substrate, creating a shear strain at the area where the light spot stays:

$$S = \frac{\delta l_t - \delta l_s}{l} \frac{w_0}{d} \quad (11)$$

where w_0 is the beam radius, d is the thickness of the full coating layer, and $\delta l_t/l, \delta l_s/l$ are the strains in the top and substrate layers, respectively. This shear strain could lower the symmetry of the crystal system from cubic to triclinic [30], thus producing a non-zero p_{63} . The value of p_{63} needs to be measured by further experiments, and in this paper we temporarily use 1% of the photoelastic coefficient p_{13} to demonstrate the influence of this effect.

B. Light penetration in multi-layer coating

The conventional structure of a low-loss mirror coating, depicted in Fig.,1, consists of N pairs of layers with high and low refractive index. The thickness of most coating layers is $\lambda/4$, except for the top layer which has a thickness of $\lambda/2$. To compute the light field reflected from the mirror coating, we adopt a method similar to that employed by LIGO in calculating thermorefringent noise,[25]. Commencing with transfer matrices for a unit cell, we deduce the matrix representing the fluctuations in the optical field reflected from the mirror coating.

1. Transfer Matrix of a unit cell

As mentioned above, mirror coating consists of repeating pairs of high and low refractive coating index layers, we denote the propagation matrix of the i th layer pair as a unit cell propagation matrix Φ_i . A unit cell is composed of two layers and two interfaces between them. A 4-dimensional vector is used to represent the light propagating through the coating:

$$\mathbf{E} = \begin{bmatrix} E_{x+} \\ E_{x-} \\ E_{y+} \\ E_{y-} \end{bmatrix}, \quad (12)$$

where x, y is the direction of polarization, \pm represent the (right/left) direction of light propagation.

The propagation matrix in the bulk medium is

$$\mathbf{T}^{(I)} = \begin{bmatrix} \mathbf{T}_x^{(I)} & 0 \\ 0 & \mathbf{T}_y^{(I)} \end{bmatrix}, \quad (13)$$

where superscript I denoted the material ($I = 1/2$ represents the SiO_2 and Ta_2O_5). $\mathbf{T}_x^{(I)}$ and $\mathbf{T}_y^{(I)}$ are the propagating matrix of the electric field $E_{x/y}$ with the coordinate system using basis vector $\mathbf{v}_1, \mathbf{v}_2$ (in [25], these two

vectors are defined as ‘‘coordinate vectors’’), which is the same in Eqs.(7) and (8), $\mathbf{T}_a^{(I)}$ is

$$\mathbf{T}_a^{(I)} = \begin{bmatrix} e^{-in_a^{(I)}kd_i^{(I)}} & 0 \\ 0 & e^{in_a^{(I)}kd_i^{(I)}} \end{bmatrix}, \quad (14)$$

where $n_a^{(I)}$ is the refractive index in the material I along the a -direction, k is the wave vector of the incident light, $d_i^{(I)}$ is the thickness of the material I in i -th layer. Since the coordinate vectors of a layer fluctuate by an angle $\delta\theta$, which is obtained by Eq.(9):

$$\delta\theta = \begin{cases} -\frac{p_{63}^{(1)}n_1^4}{n_1^2 - (n_1 + \Delta n_1)^2} \frac{\delta d_i^{(1)}}{d_i^{(1)}}, & \delta d_i^{(I)} = \delta d_i^{(1)} \\ \frac{p_{63}^{(2)}n_2^4}{n_2^2 - (n_2 + \Delta n_2)^2} \frac{\delta d_i^{(2)}}{d_i^{(2)}}, & \delta d_i^{(I)} = \delta d_i^{(2)} \end{cases}. \quad (15)$$

where the $\delta d_i^{(I)}$ represent the deformation of the material I layer in the i -th unit cell. Here we denote the optical anisotropy using the difference of refractive index along x/y directions $n_y^I = n_x^I + \Delta n_I$ and we have $\Delta n_I/n_x^I \ll 1$. The $\mathbf{R}^{(IJ)}$ is the transfer matrix of the interface between material I and J , which is combined by a rotation matrix and the transfer matrix:

$$\mathbf{R}^{(12)} = \begin{bmatrix} \mathbf{r}_{xx}^{(12)} \cos(\delta\theta) & -\mathbf{r}_{xy}^{(12)} \sin(\delta\theta) \\ \mathbf{r}_{yx}^{(12)} \sin(\delta\theta) & \mathbf{r}_{yy}^{(12)} \cos(\delta\theta) \end{bmatrix}, \quad (16)$$

$$\mathbf{R}^{(21)} = \begin{bmatrix} \mathbf{r}_{xx}^{(21)} \cos(\delta\theta) & \mathbf{r}_{xy}^{(21)} \sin(\delta\theta) \\ -\mathbf{r}_{yx}^{(21)} \sin(\delta\theta) & \mathbf{r}_{yy}^{(21)} \cos(\delta\theta) \end{bmatrix}, \quad (17)$$

where $\mathbf{r}_{ab}^{(IJ)}$ is transfer matrix of interface without considering the polarization(both sides in same polarization direction):

$$\mathbf{r}_{ab}^{(IJ)} = \frac{1}{2} \begin{bmatrix} 1 + \frac{n_b^{(J)}}{n_a^{(I)}} & 1 - \frac{n_b^{(J)}}{n_a^{(I)}} \\ 1 - \frac{n_b^{(J)}}{n_a^{(I)}} & 1 + \frac{n_b^{(J)}}{n_a^{(I)}} \end{bmatrix}, \quad (18)$$

which is described by the boundary conditions derived from Maxwell’s equation [25].

As we shall see in the next section (Eq. (21) (22)). To the first order of the strain deformation, the contributions of different layers to the propagation matrix are independent of each other, and the strain-modification of the full propagation matrix can be obtained by adding the contributions of all layers. Therefore, the key component of our calculation is the strain-modification of a single layer. In the upper panel of schematic diagram of coating cell Fig.2, the strain deformation δd_i of the layer $d_i^{(1)}$ can influence the interfaces with two neighbouring layers marked as solid line, and they are both included in the unit cell Φ_i . However, for the layer $d_i^{(2)}$, only one interface is included in the unit cell which means that another definition is needed to calculate the influence of

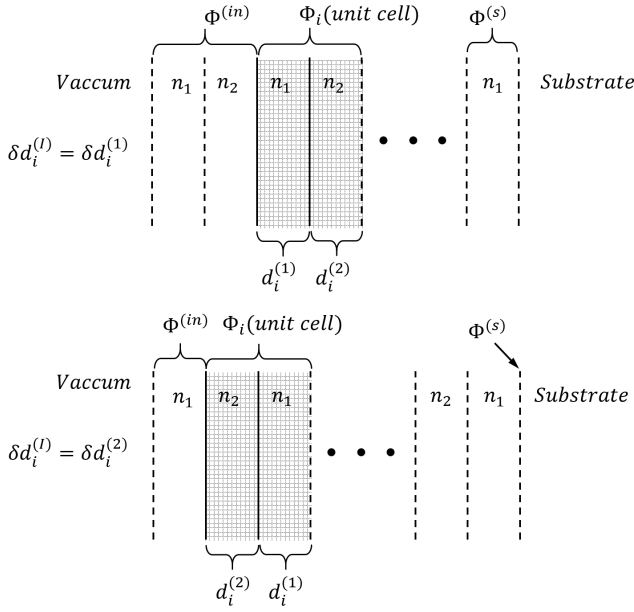


FIG. 2: Definition of the unit cell, the incident cell and the substrate cell when calculating different material coating layer. The unit cell is marked with shadows and solid lines.

$\delta d_i^{(2)}$. Therefore, it is convenient to use two different definitions for calculating $\delta d_i^{(1)}$ and $\delta d_i^{(2)}$:

$$\Phi_i = \begin{cases} \mathbf{R}^{(21)}\mathbf{T}^{(1)}\mathbf{R}^{(12)}\mathbf{T}^{(2)} & \text{when } \delta d_i^{(I)} = \delta d_i^{(1)} \\ \mathbf{R}^{(12)}\mathbf{T}^{(2)}\mathbf{R}^{(21)}\mathbf{T}^{(1)} & \text{when } \delta d_i^{(I)} = \delta d_i^{(2)} \end{cases} \quad (19)$$

The choice of the definition of Φ_i depends on the material I of the layer being calculated, which is presented in detail in next section (Section II B 2).

2. Transfer Matrix of full coating layers

The matrix of the full coating layers can be written as the product of unit cell matrices:

$$\mathbf{M} = \Phi^{(in)} \left(\prod_{i=2}^N \Phi_i \right) \Phi^{(s)}, \quad (20)$$

$$\Phi_{xy} = \Phi_{yx} \approx \begin{cases} \begin{bmatrix} \frac{p_{63}^{(1)} n_1}{4n_2 d_i^{(1)}} \left[n_2^2 - n_1^2 + i\pi n_1 n_2 \right] & n_1^2 + n_2^2 \\ n_1^2 + n_2^2 & n_2^2 - n_1^2 - i\pi n_1 n_2 \end{bmatrix}, & \delta d_i^{(I)} = \delta d_i^{(1)} \\ \frac{p_{63}^{(2)} n_2}{4n_1 d_i^{(2)}} \begin{bmatrix} n_1^2 - n_2^2 + i\pi n_1 n_2 & n_1^2 + n_2^2 \\ n_1^2 + n_2^2 & n_1^2 - n_2^2 - i\pi n_1 n_2 \end{bmatrix}, & \delta d_i^{(I)} = \delta d_i^{(2)} \end{cases}. \quad (28)$$

The definition of the incident cell $\Phi^{(in)}$ and the substrate cell $\Phi^{(s)}$ are also different when calculating different ma-

terial layers: where Φ_i represent the matrix of i -th unit cell, $\Phi^{(in,s)}$ is the propagation matrix of the incident cell and the last coating cell near the substrate, N represents the number of unit cells in the coating. Separating a unit cell matrix into the steady part and the fluctuating part:

$$\Phi_i = \Phi_0 + \Phi' \delta d_i^{(I)}. \quad (21)$$

Since $\delta d_i^{(I)}$ of different layers are independent of each other [14], their influence on \mathbf{M} can be calculated separately (except for the first and last layer):

$$\mathbf{M}(\delta d_i^{(I)}) = \Phi_0^{(in)} \Phi_0^{i-1} (\Phi_0 + \Phi' \delta d_i^{(I)}) \Phi_0^Q \Phi_0^{(s)}, \quad (22)$$

where

$$Q = \begin{cases} N - i - 2, & \delta d_i^{(I)} = \delta d_i^{(1)} \\ N - i - 1, & \delta d_i^{(I)} = \delta d_i^{(2)} \end{cases} \quad (23)$$

The definition choice of $\Phi^{(in)}$, $\Phi^{(s)}$ and Φ_i depends on the material of the fluctuating layer $\delta d_i^{(I)}$ that need to be calculated. For the fluctuation of the top layer $\delta d_1^{(1)}$ and the layer next to the substrate $\delta d_{N+1}^{(1)}$, the \mathbf{M} is:

$$\mathbf{M}(\delta d_1^{(1)}) = (\Phi_0^{(in)} + \Phi'^{(in)} \delta d_1^{(1)}) \Phi_0^{N-1} \Phi_0^{(s)}, \quad (24)$$

$$\mathbf{M}(\delta d_{N+1}^{(1)}) = \Phi_0^{(in)} \Phi_0^{N-1} (\Phi_0^{(s)} + \Phi'^{(s)} \delta d_{N+1}^{(1)}). \quad (25)$$

Using the definition in Eqs.(13-19), it turns out that Φ_0 is block-diagonal and Φ' is off-diagonal (to the first order of $\delta d_i^{(I)}$):

$$\Phi_i = \begin{bmatrix} \Phi_{xx} & 0 \\ 0 & \Phi_{yy} \end{bmatrix} + \begin{bmatrix} 0 & \Phi_{xy} \\ \Phi_{yx} & 0 \end{bmatrix} \delta d_i^{(I)}, \quad (26)$$

where Φ_{xx} and Φ_{xy} is

$$\Phi_{xx} = \Phi_{yy} \approx \begin{cases} -\frac{1}{2n_1 n_2} \begin{bmatrix} n_1^2 + n_2^2 & n_2^2 - n_1^2 \\ n_2^2 - n_1^2 & n_1^2 + n_2^2 \end{bmatrix}, & \delta d_i^{(I)} = \delta d_i^{(1)} \\ -\frac{1}{2n_1 n_2} \begin{bmatrix} n_1^2 + n_2^2 & n_1^2 - n_2^2 \\ n_1^2 - n_2^2 & n_1^2 + n_2^2 \end{bmatrix}, & \delta d_i^{(I)} = \delta d_i^{(2)} \end{cases}, \quad (27)$$

terial layers:

$$\begin{aligned}\Phi^{(in)} &= \begin{cases} \mathbf{R}^{(01)}\mathbf{T}^{(1)}\mathbf{R}^{(12)}\mathbf{T}^{(2)}, & \delta d_i^{(I)} = \delta d_1^{(1)} \\ \mathbf{R}^{(01)}\mathbf{T}^{(1)}, & \delta d_i^{(I)} = \delta d_1^{(2)} \end{cases}, \quad (29) \\ \Phi^{(s)} &= \begin{cases} \mathbf{R}^{(21)}\mathbf{T}^{(1)}\mathbf{R}^{(1s)}, & \delta d_i^{(I)} = \delta d_{N+1}^{(1)} \\ \mathbf{R}^{(1s)}, & \delta d_i^{(I)} = \delta d_{N+1}^{(2)} \end{cases}. \quad (30)\end{aligned}$$

Assuming that incident light comes from the vacuum where $n_0 = 1$, the matrix of the incident cell and the substrate cell is:

$$\Phi^{(in)} = \begin{bmatrix} \Phi_{xx}^{(in)} & \Phi_{xy}^{(in)} \delta d_1^{(1)} \\ \Phi_{yx}^{(in)} \delta d_1^{(1)} & \Phi_{yy}^{(in)} \end{bmatrix}, \quad (31)$$

$$\Phi^{(s)} = \begin{bmatrix} \Phi_{xx}^{(s)} & \Phi_{xy}^{(s)} \delta d_{N+1}^{(I)} \\ \Phi_{yx}^{(s)} \delta d_{N+1}^{(I)} & \Phi_{yy}^{(s)} \end{bmatrix}, \quad (32)$$

in which

$$\Phi_{xy}^{(in)} = \Phi_{yx}^{(in)} \approx \begin{cases} \frac{p_{63}^{(1)} n_1}{4d_1^{(1)}} \begin{bmatrix} n_1^2 - n_2 - \frac{i\pi}{2} n_1(n_2 + 1) & -n_1^2 - n_2 - \frac{i\pi}{2} n_1(n_2 - 1) \\ -n_1^2 - n_2 + \frac{i\pi}{2} n_1(n_2 - 1) & n_1^2 - n_2 + \frac{i\pi}{2} n_1(n_2 + 1) \end{bmatrix}, & \delta d_i^{(I)} = \delta d_1^{(1)} \\ 0, & \delta d_i^{(I)} = \delta d_1^{(2)} \end{cases}, \quad (35)$$

$$\Phi_{xy}^{(s)} = \Phi_{yx}^{(s)} \approx \begin{cases} \frac{p_{63}^{(1)} n_1}{8d_{N+1}^{(1)}} \begin{bmatrix} -2i(n_1^2 - n_2 n_s) - n_1(n_2 + n_s)\pi & -2i(n_1^2 + n_2 n_s) + n_1(n_s - n_2)\pi \\ 2i(n_1^2 + n_2 n_s) + n_1(n_s - n_2)\pi & 2i(n_1^2 - n_2 n_s) - n_1(n_2 + n_s)\pi \end{bmatrix}, & \delta d_i^{(I)} = \delta d_{N+1}^{(1)} \\ 0, & \delta d_i^{(I)} = \delta d_{N+1}^{(2)} \end{cases} \quad (36)$$

where the n_s is the refractive index of substrate (usually made by SiO_2). Note that Δn_1 and Δn_2 in Eqs.(27)-(36) is neglected since $\Delta n_I/n_x^I \ll 1$.

3. The reflected light from the coating layers

The entire coating layers can be described as a 4×4 matrix \mathbf{M} , connecting the optical field on the right of the coating to those on the left:

$$\begin{bmatrix} E_{in} \\ E_{rx} \\ 0 \\ E_{ry} \end{bmatrix} = \begin{bmatrix} M_{11} & M_{12} & M_{13} & M_{14} \\ M_{21} & M_{22} & M_{23} & M_{24} \\ M_{31} & M_{32} & M_{33} & M_{34} \\ M_{41} & M_{42} & M_{43} & M_{44} \end{bmatrix} \begin{bmatrix} E_{tx} \\ 0 \\ E_{ty} \\ 0 \end{bmatrix}, \quad (37)$$

where E_{in} is incident light polarized along x-axis, E_{rx}, E_{ry} is the light field reflected by the coating layers, E_{tx}, E_{ty} is the transmitted light. Since we are interested in the variation of the polarization state, the only term that needs to be calculated is E_{ry} :

$$r_y = \frac{E_{ry}}{E_{in}} = \frac{M_{41}M_{33} - M_{43}M_{31}}{M_{11}M_{33} - M_{13}M_{31}}, \quad (38)$$

which is obtained by solving Eq.(37). The real part of r_y represents the change in polarization angle, and the

$$\begin{aligned}\Phi_{xx}^{(in)} &= \Phi_{yy}^{(in)} \\ &\approx \begin{cases} -\frac{1}{2n_1} \begin{bmatrix} n_1^2 + n_2^2 & n_2^2 - n_1^2 \\ n_2^2 - n_1^2 & n_1^2 + n_2^2 \end{bmatrix}, & \delta d_i^{(I)} = \delta d_i^{(1)} \\ \frac{i}{2} \begin{bmatrix} -1 - n_1 & 1 - n_1 \\ -1 + n_1 & 1 + n_1 \end{bmatrix}, & \delta d_i^{(I)} = \delta d_i^{(2)} \end{cases}, \quad (33)\end{aligned}$$

and

$$\begin{aligned}\Phi_{xx}^{(s)} &= \Phi_{yy}^{(s)} \\ &\approx \begin{cases} \frac{i}{2n_1 n_2} \begin{bmatrix} -n_1^2 - n_2 n_s & -n_1^2 + n_2 n_s \\ n_1^2 - n_2 n_s & n_1^2 + n_2 n_s \end{bmatrix}, & \delta d_i^{(I)} = \delta d_{N+1}^{(1)} \\ \frac{1}{2} \begin{bmatrix} 1 + n_s/n_1 & 1 - n_s/n_1 \\ 1 - n_s/n_1 & 1 + n_s/n_1 \end{bmatrix}, & \delta d_i^{(I)} = \delta d_{N+1}^{(2)} \end{cases}, \quad (34)\end{aligned}$$

imaginary part represents the change in ellipticity (i.e., birefringence). It turns out that most of the r_y is the imaginary part (see Section III) so that the real part can be neglected. The transfer matrix \mathbf{M} describes the response of the light field with respect to the coating surface, therefore \mathbf{M} depends on the rotation angle of the optical axis $\delta\theta$. Furthermore, the $\delta\theta$ is related to δd by Eq.(9), which leads to a relationship between the ellipticity fluctuations spectrum S_ψ and the deformation spectrum of a single coating layer $S_{d_i^{(I)}}$:

$$S_\psi^{1/2} = \sqrt{\sum_{I=1}^2 \sum_{i=1}^N \left(\frac{\partial r_y}{\partial d_i^{(I)}} \right)^2 S_{d_i^{(I)}}}. \quad (39)$$

The fluctuation of the coating layer thickness $\delta d_i^{(I)}$ is typically a Brownian type thereby showing a Brownian spectrum of S_ψ . Note that the summation is over the influence of different layers. We do not have the cross term like $S_{d_i^{(I)} d_j^{(J)}}$ is because that the deformations caused by Brownian motion in the different layers are independent of each other[14].

TABLE I: Typical parameters used in this paper.

Parameters	Symbol	GaAs	AlGaAs
Refractive index	n	3.37[31]	2.90[32]
Poisson's ratio	σ		0.32[31]
Young's modulus(GPa)	Y		100[23]
Loss angle	ϕ		2.41×10^{-5} [33]
Temperature(K)	T		293
Beam radius(μm)	r_0		1500
Photoelastic coefficient	p_{13}	-0.14[34]	
Photoelastic coefficient	p_{63}	-0.0014	

III. CALCULATED NOISE LEVEL

In this section we present the noise level of the non-diagonal anisotropic Brownian photoelastic (NABP) effect using the parameters listed in Table I, based on the theory established in Section II. As mentioned in Section II A, the p_{63} in the crystalline coating materials may arise from strain induced during the deposition process, and there is currently no experimental measurement of p_{63} in the coating material. On the other hand, the theoretical quantitative estimation of p_{63} requires a first-principle density-functional calculation [35, 36]. In this paper, we focus on demonstrating the influence of the non-diagonal anisotropic Brownian photoelastic effect, and the value of $p_{63} = -0.0014$ is assumed to be one percent of p_{13} and the values of p_{63} in both coating materials are assumed to be the same. The real value of p_{63} could be smaller than this assumption, which needs to be determined by further experimental test or more detailed density-functional calculation by the material science theorists.

One can derive a complete expression for the \mathbf{M} -matrix by substituting Eqs.(21-36) into Eq.(20). The contribution of the different layers to the ellipticity ($\partial r_y / \partial d_i$) is then obtained by Eq.(38), as shown in Fig.3. We can see that the effect of the layer on the ellipticity decreases as the number of layers increases, so that only the first few layers contribute most to the variation of the ellipticity.

For a single coating layer, the thickness fluctuation due to the Brownian motion is obtained using Levin's approach [12, 14]:

$$S_d(f) = \frac{8k_B T d_i \phi_i (1 - \sigma_i - 2\sigma_i^2)}{3\pi^2 f Y_i (1 - \sigma_i)^2 r_0^2}, \quad (40)$$

where k_B is the Boltzmann constant, d_i is the thickness of this layer, ϕ_i is the loss angle, σ_i is Poisson's ratio, Y_i is Young's modulus, r_0 is the radius of the laser beam.

The noise level of the NABP effect is obtained by substituting Eq.(40) into Eq.(39), as shown in Fig.4. This result demonstrates that, using the sampled parameters

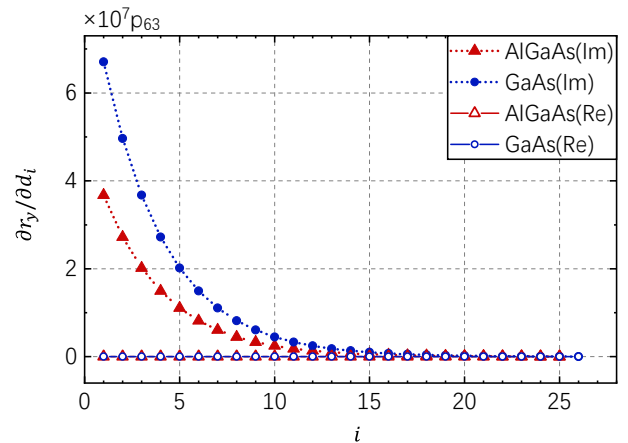


FIG. 3: Influence of different layer thicknesses on the ellipticity for a 19 pairs of GaAs/AlGaAs coated mirror. As previously mentioned, the imaginary part of $\partial r_y / \partial d_i$ represents the change in ellipticity of the light reflected from the mirror and the real part represents the change in polarization angle. The real part of $\partial r_y / \partial d_i$ is four orders of magnitude smaller than the imaginary part thereby can be ignored.

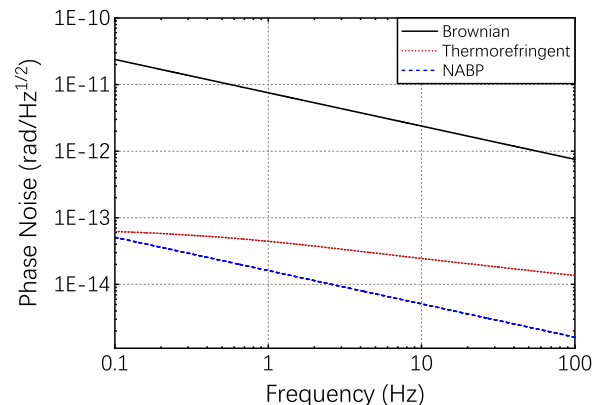


FIG. 4: Non-diagonal anisotropic Brownian photoelastic noise (NABP) calculated for an 25-pair GaAs/AlGaAs coated mirror. The comparison with the Brownian noise and thermorefringent noise is also shown.

for the p_{63} in Table I, the NABP noise is

$$S_{\psi(NABP)}^{1/2} = 1.2 \times 10^{-11} p_{63} f^{-1/2} / \sqrt{\text{Hz}}, \quad (41)$$

which is shown in Fig.4, and the Brownian noise and the thermorefringent noise are also shown for comparison. Here the thermorefringent noise is [25]:

$$S_{\psi(TF)} = \left| r_y \frac{\pi}{2} \frac{n_2 \varepsilon_{xy}^{(1)} + n_1 \varepsilon_{xy}^{(2)}}{n_1 n_2 (n_1^2 - n_2^2)} \right|^2 S_{uu}(f), \quad (42)$$

where $\varepsilon'_{xy} = 10\text{ppm/K}$ is thermorefractive coefficient, r_y is reflection amplitude for y -polarization and S_{uu} is the power spectral density of temperature averaged over the

beam spot:

$$S_{uu}(f) = \frac{2k_B T^2}{\pi r_0 c_V D} \operatorname{Re} \left\{ \int_0^\infty du \frac{u e^{-u^2/2}}{\sqrt{u^2 - i r_0^2 f/D}} \right\}, \quad (43)$$

where $c_V = 1.6 \times 10^6 \text{J(mK)}^{-1}$ is heat capacity per unit volume, $\kappa = 1.38 \text{W(mK)}^{-1}$ is the thermal conductivity and $D = \kappa/c_V$ is thermal diffusivity.

IV. CONCLUSIONS

For experiments such as the measurement of vacuum magnetic birefringence, the measurement principle is to amplify the signal through a resonant cavity, which is then detected by a polarimetry. This polarimetry detects the phase difference between the two polarization directions, so that the phase noise is cancelled out. Thus, the sensitivity of these experiments is not limited by the commonly discussed thermal phase noise (Brownian, thermo-optic noise) but by the thermal birefringent noise. Experimental measurements and theoretical investigations of the anisotropy of these coating materials are important.

In this work, we present a comprehensive analysis of a novel kind of birefringent noise induced by the Brownian motion of the mirror coating. In particular, we discussed the possible influence of a novel noise source originating from the non-diagonal anisotropic photoelastic effect, which may limited the sensitivity of precision polarimetry experiments. The strain deformation caused by Brownian motion in a single coating layer induces a rotation of the intrinsic birefringence due to the non-diagonal anisotropic photoelastic effect. By extending these findings to multilayer surfaces using the matrix method, we elucidate the corresponding fluctuations in the light reflected from the mirror.

For the GaAs-AlGaAs coating, the noise level

caused by the non-diagonal anisotropic Brownian photoelastic (NABP) effect is calculated to be $1.2 \times 10^{-11} p_{63} f^{-1/2} / \text{Hz}^{1/2}$ using the sampled parameters in Table I. The non-diagonal anisotropic Brownian photoelastic noise level is decisively dependent on the value of p_{63} . Assuming that p_{63} is one percent of the p_{13} , the NABP noise level is of the same order of magnitude as the thermorefringent noise. In addition, the anisotropy in the different parts of the coating can introduce loss in reflectivity [29]. This will generate noise according to the fluctuation-dissipation theorem, which could be a stronger effect than the NABP noise effect. This anisotropy can be evaluated through measuring the intrinsic birefringence of different parts of the coating surface, hence further compensated probably. The source of the p_{63} and other anisotropies of the coating materials could be the strain induced during the manufacturing process, the specific mechanisms and the evaluation of p_{63} for the coating material require further experimental and theoretical investigation.

ACKNOWLEDGMENTS

The authors thank Professor Chunnong Zhao, Dr. Haoyu Wang, Dr. Serhii Kryhin and Dr. Evan D. Hall for very helpful discussions. They also want to thank the anonymous referees for giving very useful suggestions to improve our manuscript. In addition, the authors also thank Dr. Lin Zhu and other members of the MOE Key Laboratory of Fundamental Physical Quantities Measurement for useful discussions. This work is supported by the the National Key R&D Program of China (2023YFC2205801), National Natural Science Foundation of China under Grant Nos.12150012,12175317,11925503.

-
- [1] G. M. Harry, A. M. Gretarsson, P. R. Saulson, S. E. Kittelberger, S. D. Penn, W. J. Startin, S. Rowan, M. M. Fejer, D. Crooks, G. Cagnoli, *et al.*, Thermal noise in interferometric gravitational wave detectors due to dielectric optical coatings, *Classical and Quantum Gravity* **19**, 897 (2002).
- [2] A. E. Villar, E. D. Black, R. DeSalvo, K. G. Libbrecht, C. Michel, N. Morgado, L. Pinard, I. M. Pinto, V. Pierro, V. Galdi, *et al.*, Measurement of thermal noise in multilayer coatings with optimized layer thickness, *Physical Review D* **81**, 122001 (2010).
- [3] T. Chalermsoongsak, F. Seifert, E. D. Hall, K. Arai, E. K. Gustafson, and R. X. Adhikari, Broadband measurement of coating thermal noise in rigid fabry-pérot cavities, *Metrologia* **52**, 17 (2014).
- [4] S. Gras, H. Yu, W. Yam, D. Martynov, and M. Evans, Audio-band coating thermal noise measurement for advanced ligo with a multimode optical resonator, *Physical Review D* **95**, 022001 (2017).
- [5] M. Granata, A. Amato, G. Cagnoli, M. Coulon, J. Degallaix, D. Forest, L. Mereni, C. Michel, L. Pinard, B. Sassolas, *et al.*, Progress in the measurement and reduction of thermal noise in optical coatings for gravitational-wave detectors, *Applied optics* **59**, A229 (2020).
- [6] K. Numata, M. Ando, K. Yamamoto, S. Otsuka, and K. Tsubono, Wide-band direct measurement of thermal fluctuations in an interferometer, *Physical review letters* **91**, 260602 (2003).
- [7] K. Numata, A. Kemery, and J. Camp, Thermal-noise limit in the frequency stabilization of lasers with rigid cavities, *Physical review letters* **93**, 250602 (2004).
- [8] M. Notcutt, L.-S. Ma, A. D. Ludlow, S. M. Foreman, J. Ye, and J. L. Hall, Contribution of thermal noise to frequency stability of rigid optical cavity via hertz-linewidth

- lasers, *Physical Review A* **73**, 031804 (2006).
- [9] D. Matei, T. Legero, S. Häfner, C. Grebing, R. Weyrich, W. Zhang, L. Sonderhouse, J. Robinson, J. Ye, F. Riehle, *et al.*, 1.5 μ m lasers with sub-10 mhz linewidth, *Physical review letters* **118**, 263202 (2017).
- [10] Z. Ma, H. Liu, W. Wei, W. Yuan, P. Hao, Z. Deng, H. Che, Z. Xu, F. Cheng, Z. Wang, *et al.*, Investigation of experimental issues concerning successful operation of quantum-logic-based 27 al⁺ ion optical clock, *Applied Physics B* **126**, 129 (2020).
- [11] J. Yu, S. Häfner, T. Legero, S. Herbers, D. Nicolodi, C. Y. Ma, F. Riehle, U. Sterr, D. Kedar, J. M. Robinson, *et al.*, Excess noise and photoinduced effects in highly reflective crystalline mirror coatings, *Physical Review X* **13**, 041002 (2023).
- [12] Y. Levin, Internal thermal noise in the ligo test masses: A direct approach, *Physical Review D* **57**, 659 (1998).
- [13] M. Evans, S. Ballmer, M. Fejer, P. Fritschel, G. Harry, and G. Ogin, Thermo-optic noise in coated mirrors for high-precision optical measurements, *Physical Review D* **78**, 102003 (2008).
- [14] T. Hong, H. Yang, E. K. Gustafson, R. X. Adhikari, and Y. Chen, Brownian thermal noise in multilayer coated mirrors, *Physical Review D* **87**, 082001 (2013).
- [15] R. Cameron, G. Cantatore, A. Melissinos, G. Ruoso, Y. Semertzidis, H. Halama, D. Lazarus, A. Prodell, F. Nezzrick, C. Rizzo, *et al.*, Search for nearly massless, weakly coupled particles by optical techniques, *Physical Review D* **47**, 3707 (1993).
- [16] A. Ejlli, F. Della Valle, U. Gastaldi, G. Messineo, R. Pengo, G. Ruoso, and G. Zavattini, The pvlas experiment: A 25 year effort to measure vacuum magnetic birefringence, *Physics Reports* **871**, 1 (2020).
- [17] X. Fan, S. Kamioka, T. Inada, T. Yamazaki, T. Namba, S. Asai, J. Omachi, K. Yoshioka, M. Kuwata-Gonokami, A. Matsuo, *et al.*, The oval experiment: a new experiment to measure vacuum magnetic birefringence using high repetition pulsed magnets, *The European Physical Journal D* **71**, 1 (2017).
- [18] J. Agil, R. Battesti, and C. Rizzo, Vacuum birefringence experiments: optical noise, *The European Physical Journal D* **76**, 192 (2022).
- [19] S.-J. Chen, H.-H. Mei, and W.-T. Ni, Q & a experiment to search for vacuum dichroism, pseudoscalar-photon interaction and millicharged fermions, *Modern Physics Letters A* **22**, 2815 (2007).
- [20] K. Ehret, M. Frede, S. Ghazaryan, M. Hildebrandt, E.-A. Knabbe, D. Kracht, A. Lindner, J. List, T. Meier, N. Meyer, *et al.*, New alps results on hidden-sector lightweights, *Physics Letters B* **689**, 149 (2010).
- [21] H. Liu, B. D. Elwood, M. Evans, and J. Thaler, Searching for axion dark matter with birefringent cavities, *Physical Review D* **100**, 023548 (2019).
- [22] I. Obata, T. Fujita, and Y. Michimura, Optical ring cavity search for axion dark matter, *Physical review letters* **121**, 161301 (2018).
- [23] G. D. Cole, W. Zhang, M. J. Martin, J. Ye, and M. Aspelmeyer, Tenfold reduction of brownian noise in high-reflectivity optical coatings, *Nature Photonics* **7**, 644 (2013).
- [24] T. Chalermongsak, E. D. Hall, G. D. Cole, D. Follman, F. Seifert, K. Arai, E. K. Gustafson, J. R. Smith, M. Aspelmeyer, and R. X. Adhikari, Coherent cancellation of photothermal noise in gaas/al0.92ga0.08as bragg mirrors, *Metrologia* **53**, 860 (2016).
- [25] S. Kryhin, E. D. Hall, and V. Sudhir, Thermorefringent noise in crystalline optical materials, *Physical Review D* **107**, 022001 (2023).
- [26] N. Kondratiev, A. Gurkovsky, and M. Gorodetsky, Thermal noise and coating optimization in multilayer dielectric mirrors, *Physical Review D* **84**, 022001 (2011).
- [27] G. Harry, T. P. Bodiya, and R. DeSalvo, *Optical coatings and thermal noise in precision measurement* (Cambridge University Press, 2012).
- [28] A. Yariv and P. Yeh, *Optical waves in crystal propagation and control of laser radiation*, (1983).
- [29] S. Vyatchanin, The loss in reflecting coating induced by polarization, *Physics Letters A* **384**, 126878 (2020).
- [30] Y. Sun, S. E. Thompson, and T. Nishida, *Strain effect in semiconductors: theory and device applications* (Springer Science & Business Media, 2009).
- [31] S. Adachi, *Properties of aluminium gallium arsenide*, 7 (IET, 1993).
- [32] M. A. Afromowitz, Refractive index of ga1-xalx, *Solid State Communications* **15**, 59 (1974).
- [33] G. D. Cole, I. Wilson-Rae, K. Werbach, M. R. Vanner, and M. Aspelmeyer, Phonon-tunnelling dissipation in mechanical resonators, *Nature communications* **2**, 231 (2011).
- [34] R. Dixon, Photoelastic properties of selected materials and their relevance for applications to acoustic light modulators and scanners, *Journal of Applied Physics* **38**, 5149 (1967).
- [35] F. Detraux and X. Gonze, Photoelasticity of α -quartz from first principles, *Physical Review B* **63**, 115118 (2001).
- [36] D. Donadio, M. Bernasconi, and F. Tassone, Photoelasticity of crystalline and amorphous silica from first principles, *Physical Review B* **68**, 134202 (2003).